Neutrality for Sustainability: The Promise of Neutral Hosts for Sustainable Mobile Networks

Boris Gerretzen and Suzan Bayhan
University of Twente, Enschede, The Netherlands
suzan.bayhan@utwente.nl

***Abstract*—Mobile networks have become an essential pillar in a nation's critical digital infrastructure meeting the connectivity and communication needs of various sectors. To meet the increasing demands, e.g., on data rates and the regulatory requirements on coverage, each mobile network operator (MNO) deploys its infrastructure (namely base stations, BSs) densely, most of the time resulting in a mobile user receiving signals with high quality from many BSs. Moreover, typically there are multiple competing MNOs in a country deploying their infrastructure separately. While a high density of BSs is desirable for serving users with high satisfaction and also for the resiliency of the network, it raises a question on the associated environmental footprint. As a potential solution, this paper investigates the gains unlocked by *neutral host networks* (NHNs) on the sustainability of the national cellular infrastructure in terms of power consumption and carbon emissions. An NHN is a third-party owning the physical infrastructure and leasing it to MNOs on a shared basis. Our data-driven analysis[1] using the telecom data in the Netherlands suggest that the carbon emission related to radio access network of the nation-wide cellular infrastructure can be decreased noticeably, e.g., ∼28% to ∼41% depending on the scenario, by the help of an NHN owing to the decreased redundant deployment and higher utilization of existing infrastructure leading to lower waste due to the idle power of the BSs.**

***Index Terms*—Sustainability, mobile networks, neutral hosts.**

I. Introduction

Mobile connectivity has become indispensable for every day operation of citizens and industries alike. This wide adoption is due to not only the significant technological advances in the past decade, e.g., from 4G to 5G, but also a very dense deployment of the telecoms infrastructure and its over-provisioning to accommodate for any traffic burst or potential disruptions, e.g., due to planned maintenance. It is typical that a mobile device receives signals with high signal-quality from many base stations (BS) as shown in Fig.1 and BSs are reportedly underutilized most of the time, e.g., with average load on the busiest hours varying from 8-28% [2]. This low utilization and high-quality signal coverage points to the redundancy in the telecoms infrastructure which is necessary for the resiliency of this critical infrastructure. However, despite their low utilization, the power consumption of the BSs and associated equipment, referred to as radio access network (RAN), accounts for the highest fraction of a mobile network operator's (MNO) power consumption, e.g., more than 50% [3]. Hence, in the realm of climate crises and the urgency of decreasing the emissions, the tradeoff between the degree of redundancy and associated environmental cost must be revisited.

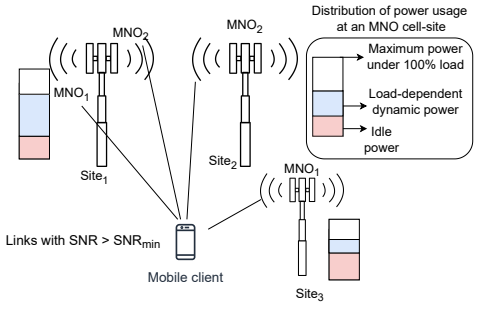

Fig. 1: Mobile networks are deployed ubiquitously resulting in high signal quality (represented as SNR) at a mobile client from many BSs. Consequently, average load at each BS is typically low whereas the power consumption is not as low due to the non-negligible idle power consumption.

Additionally, multiple MNOs deploy their own separate networks aiming nation-wide coverage. Each MNO deploys and maintains its own BSs, backhaul links, and other infrastructure components to serve its customers. While this approach encourages competition, it also leads to inefficiencies. For example, in the Netherlands, three major MNOs operate their own networks of thousands of BSs, often located in close proximity to each other. This isolated operation increases both the financial and environmental costs associated with mobile network deployment and operation. First, the duplication of infrastructure leads to higher capital expenditures and operational costs for each MNO, as they must invest in equipment, maintenance, and upgrades for their own networks. Second, and more importantly in the context of climate change and sustainability, the redundant infrastructure results in increased energy consumption and carbon emissions. As the Information and Communication Technology (ICT) sector is estimated to account for 1.8% to 3.9% of global carbon emissions [4], with mobile networks being a significant contributor, there is a need to explore solutions that can reduce the environmental impact of mobile networks [5], [6].

To address these challenges, a concept known as *neutral host networks* (NHN) can act as a promising solution which promotes the use of a single shared infrastructure managed by a neutral entity. The neutral host operator is responsible for

[1]This paper is based on a master thesis [1], which has been extended with further analysis and discussion.

the deployment, maintenance, and operation of the network on a multi-tenancy basis, while MNOs can lease access to this shared infrastructure as tenants and focus on delivering services to their customers. As discussed in [7], there are different levels of sharing from passive components only (e.g., cell sites, power sources) to sharing of active components in the radio access network (e.g., radio equipment, spectrum) or the mobile core network. Note that passive infrastructure sharing has already been a common practice whereas active sharing has only recently gained attention.

Recent studies such as [8] show the potential of infrastructure sharing in reducing energy consumption, hence focusing on operational emissions. In contrast to these studies which focus on sharing approaches of existing MNO networks, we focus on the deployment of the shared infrastructure and its impact on total carbon emission including the embodied carbon. Although several studies such as [9]–[11] have explored the technical and economic aspects of NHNs, much of the existing research focuses on small-scale deployments or specific use cases. There is a lack of comprehensive studies that evaluate the system-level impact of a nation-wide NHN using real infrastructure data, and most importantly how they might affect carbon emissions of the national cellular infrastructure. This paper aims at filling this gap and focuses on the following research questions: *(i) How can we design an NHN that delivers adequate network performance in terms of coverage, redundancy and signal quality (SNR) on a national scale while minimizing power consumption?; and (ii) What is the resulting impact on power consumption, carbon emissions, and network performance in terms of coverage, redundancy and SNR when replacing separate MNOs with a single NHN?*

Towards addressing these questions, after reviewing the literature in Sec.II, we present our model and assumptions in Sec.III. Our methodology is presented in Sec.IV and consists of (i) data collection and preprocessing, (ii) a hypothetical NHN deployment approach to determine the locations of NHN BSs (Sec.V) and (iii) performance evaluation of an NHN in terms of energy consumption, carbon emissions, and quality of service in comparison to the current MNO operations with separate infrastructures (Sec.VI). After discussing the limitations of our work in Sec.VII, we conclude in Sec.VIII.

II. Related Work

Several prior studies have identified network sharing as an indispensable pathway to sustainability, e.g., [7], [8], [12], as infrastructure sharing facilitates consolidation of load in some BSs and putting other BSs into power-saving sleep mode during periods of low traffic activity. The closest study to ours is [7] which studies the carbon emission of an ideal scenario where the RAN becomes a common good and MNOs are fully cooperative. Using the data from France with four MNOs, authors estimate carbon savings up to 79% if MNOs operate fully cooperatively. Our study has the same goal, namely assessing the potential of such shared RAN operation. However, in addition to our study not assuming an ideal scenario requiring full cooperation, our methodology differs from [7] in that we base our calculations on a more fine grained model of RANs, e.g., user association, the theoretical capacity of a wireless link between a BS and a user, and power consumption models reflecting the power impact of utilization of a BS. Our study can be considered as a further evidence supporting the findings of [7] with a different case study, namely in the Netherlands. To decrease RAN power consumption while ensuring that mobile traffic is carried without congestion, Renga et al. [12] propose offloading traffic to certain BSs owned by any of the cooperating MNOs with co-located BSs. Authors model also the potential impact of sharing on the BS lifetime by considering both potential improvement due to lower temperature during sleep periods resulting in lower hardware failure rate and also degradation due to switching between active and sleeping states. The study based on the data from France demonstrates the effectiveness of infrastructure sharing in reducing power consumption and embodied emissions due to extended BS lifetime with cautious load consolidation. Similarly, Finarelli et al. [8] demonstrate the potential power savings to be up to 35% for a case study in France after developing an analytical framework using stochastic geometry.

Ahmed and Coupechoux [4] estimated the operational power consumption of BSs in France over the period spanning 2015 to 2022 using publicly available data combined with established power consumption models. Despite data availability limitations, the study shows sustained growth in the number of BSs and transceivers, leading to an annual increase of nearly 18% in total BS power consumption. The results point to an increase in power consumption due to 5G deployment, outweighing efficiency gains and legacy technology decommissioning. A similar study was conducted for Belgium by Golard *et al.* in [2] covering the period 2020–2025 considering various scenarios. Authors also estimate the carbon footprint of 4G and 5G networks by considering embodied and operational emissions.

A key factor in the accuracy of estimations of the total power consumption is the accuracy of power consumption models for a specific cellular technology. While all prior work agree on models that account for load-independent idle power and load-dependent dynamic power consumption, how additional factors, e.g., the number of transceivers, affect the power consumption is yet to be understood. Golard et al. [13] present a model for 5G BSs combining models, on-site measurements from operators, and with radio equipment documentation from manufacturers. While our study limits itself to 4G, using such models for 5G BSs, our study can be expanded to newer 5G deployments. A recent study by Zhong and Ge [14] presents associated carbon emissions for BS equipment and cell sites considering operational and embodied emissions and presents the steps toward carbon-neutral mobile networks. While all these studies guided us in our modeling and provided also parameters for our analysis, to the best of our knowledge, there is no comparable study on the analysis of NHNs at a national scale.

III. System Model

In this section, we overview key models and assumptions that lay the basis of our study.

A. Network model

We consider a national cellular network infrastructure consisting of multiple MNOs. We model each MNO as a set of BSs $\mathcal{B}$, each $b \in \mathcal{B}$ located at position p_b with height h_b. Each $b \in \mathcal{B}$ equipped with a set of antennas $\mathcal{A}_b \subseteq \mathcal{A}$. Each antenna $a \in \mathcal{A}$ operates in frequency band f_a and has a fixed transmit power P_a^{tx}. We assume that all BSs follow the remote radio head (RRH) architecture, where a BS consists of a baseband unit (BBU) and multiple RRHs connected via fronthaul links. We consider only downlink communication in this study as downlink is still the dominant traffic. However, our models and analysis can also be extended to uplink communications.

To represent users served by an MNO, we define a population density function $\phi(x)$ over area Ω and determine the number of users in that area. To mimic the network association which is typically based on signal quality perceived by a user, we use an area based association model to determine which BS serves which users. Using the set of BSs $\mathcal{B}$, we create a Voronoi partitioning of the area covered by the network. Each Voronoi cell corresponds to the coverage area of a BS, and users located within that cell are served by the corresponding BS. Consequently, we define the population served by each BS $b \in \mathcal{B}$ as pop_b, which is the total population located within the Voronoi cell V_b and represent it as follows: $pop_b = \int_{V_b} \phi(x)\, dx$.

B. Channel model

To reflect current MNO deployments consisting of BSs at urban and rural areas, we consider two types of channel models created by 3GPP [15], urban macro (UMa) and rural macro (RMa) which models both line-of-sight and non-line-of-sight conditions. Let us denote by $L_{a,u}$ the path loss between antenna a and user u located at distance $d_{a,u}$ from antenna a. $L_{a,u}$ is a function of the following factors: $d_{a,u}$, antenna transmission gain at the transmitter (G_{tx}) and the receiver (G_{rx}), the transmit power of the antenna (P_a^{tx}), noise power at the user antenna (N_u), carrier frequency (f_c), the average height of surrounding buildings, height of the BS and the user equipment (UE) antenna, 2D and 3D distance between the BS and the UE, speed of light, and average street width.

Each antenna a is assumed to have a fixed transmission gain G_{tx} and each user u a fixed reception gain G_{rx}. The received power $P_{a,u}^{rx}$ at user u from antenna a is calculated as:

$$P_{a,u}^{rx}[\text{dBm}] = P_a^{tx}[\text{dBm}] + G_{tx}[\text{dB}] - L_{a,u}[\text{dB}] + G_{rx}[\text{dB}]. \quad (1)$$

We model noise power N_u at user u as thermal noise plus a constant noise figure NF representing receiver imperfections using a bandwidth B_u allocated to user u:

$$N_u[\text{dBm}] = -174 + 10\log_{10}(B_u[\text{Hz}]) + NF[\text{dB}]. \quad (2)$$

Consequently, to represent the signal quality, we can calculate signal-to-noise ratio (SNR) at user u from antenna a as follows:

$$\text{SNR}_{a,u}[\text{dB}] = P_{a,u}^{rx}[\text{dBm}] - N_u[\text{dBm}]. \quad (3)$$

IV. Methodology

This section introduces our three-step methodology summarized in Fig.2, namely (i) Step-1: data collection[2] and preprocessing for constructing an MNO along with its BSs, antennas, users, and cell-areas; (ii) Step-2: network construction including NHN construction followed by user-BS association; and (iii) Step-3: performance evaluation via a set of scenario simulations to investigate the performance of each MNO and NH scenario. Next, we present each step of our methodology.

A. Step-1: Data collection and preprocessing

To represent the cellular infrastructure, the physical propagation environment, and the users, we collect data from various sources which we introduce next.

Antenna data: The primary dataset providing information about the mobile networks in the Netherlands is made publically accessible by the Dutch Rijksinspectie Digitale Infrastructuur (RDI), and it includes information on the location and specifications of BSs operating in the Netherlands.[3] The dataset is structured using two sets of data: one for the BSs and one for the antenna groups associated with those BSs. Each BS has an entry in the "Antennes" table, which includes information such as the geographic coordinates as well as the postal code and municipality, and the technologies supported by the BS (e.g., 2G, 3G, 4G, 5G). Each entry in the "Antennes" table also has a list of associated antenna groups, which are stored in the "Antenne_Groepen" table. For each technology supported by the BS, there is an entry in the "Antenne_Groepen" table, which includes information such as the frequency band, the maximum transmit power, the antenna type, and the azimuth and tilt of the antenna. Note that a single BS can have multiple antenna groups, and each antenna group is comprised of one or more entries in the "Antenne_Groepen" table. There is one entry in the "Antenne_Groepen" table for each transceiver (TRX) associated with the antenna group. Furthermore, this dataset includes information about other types of radio equipment not related to mobile networks, such as ham radio antennas and TV transmitters. To filter out only the relevant entries for mobile networks, we only consider BSs that have antenna groups associated with the 4G LTE technology. This ensures that we only include BSs that are part of the mobile networks operated by MNOs in the Netherlands. In our analysis, we focus on 4G LTE networks as 5G deployment is still in-progress. However, our methodology can be extended to 5G networks by using appropriate power and path loss models that take into account technological differences like massive MIMO [4].

As this dataset does not include information about the ownership of a BS, we cross-reference the frequencies of the antennas with the frequency allocations for each MNO [16].

[2]Please see our repository for more on data collection: https://github.com/BorisGerretzen/AntennaScraper.

[3]https://antenneregister.nl/viewer/

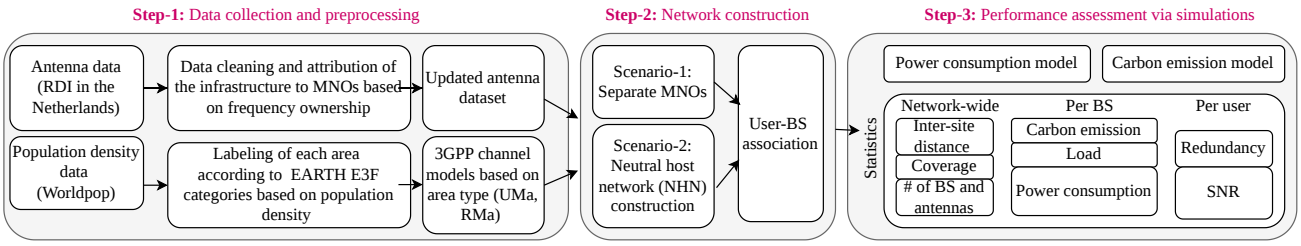

Fig. 2: Three step research methodology: Step-1 consisting of data collection and preprocessing for constructing an MNO along with its BSs, antennas, users, and cell-areas; Step-2 including network construction with user-antenna association and neutral host construction; Step-3 consisting of a set of scenario simulations to investigate the performance of each MNO and NHN.

TABLE I: EARTH E3F population density categories [18] [19].

Area Type	Population density (users/km^2)	Channel model
Super Dense Urban	$>$ 20,000	UMa
Dense Urban	3,000 - 20,000	UMa
Urban	500 - 1,000	UMa
Suburban	100 - 500	UMa
Rural	25-100	RMa
Wilderness	$<$ 25	RMa

We use this information to assign each BS to the MNO that operates all of its antennas.[4]

Population data: To represent the variations in the number of users that needs to be served across the country, we used the Worldpop dataset [17] which provides the estimated population count per square kilometer for the Netherlands.

Physical propagation environment: We classify each location in the Netherlands according to one of six types outlined by the EARTH E3F project [18] [19] based on population density (refer to Table I). After this classification, we use one of the 3GPP channel models, namely Urban macrocell (UMa) and Rural Macrocell (RMa), that can reflect the physical propagation environment.

B. Step-2: Neutral host construction and user-BS association

In this step, we model two scenarios: (i) current deployments in an isolated manner by multiple MNOs and (ii) a hypothetical NHN allowing multiple MNOs using its infrastructure. For the NHN scenario, we present our approach in Sec.V to determine the locations of the BSs owned by such an NHN along with the resources at each BS. For each scenario, we adopt the same user-BS association scheme as described in Sec.III to reflect the SNR-based association adopted in mobile networks.

C. Step-3: Performance evaluation

We evaluate a setting, e.g., an MNO or NHN scenario, using SNR distribution, coverage, redundancy, power consumption, and carbon emission, which we introduce next.

SNR model: We start by building a Voronoi partition of the network based on the BS locations. We then overlay our population density dataset on top of this Voronoi partition to calculate the population served by each BS. We also use the population dataset to classify each BS according to the EARTH E3F categories outlined in Table I, which determines the path loss model used when calculating the SNR for users served by that BS. After mapping BSs to area types, we estimate the SNR at sampled locations. Consequently, to reflect the country-wide SNR distribution, we weight each sample based on the population density of the associated area.

Coverage κ: We define coverage κ based on SNR experienced by users in the network. A user u is considered to be in coverage if the SNR from at least one antenna a serving that user exceeds a predefined threshold SNR_{min}. We formally define the coverage for a user κ_u as follows:

$$\forall u \in \mathcal{U} : \kappa_u = \begin{cases} 1 & \text{if } \exists a \in \mathcal{A} : SNR_{a,u} > \text{SNR}_{\text{min}}, \\ 0 & \text{otherwise.} \end{cases} \quad (4)$$

Letting $\mathcal{U}$ be the set of all users in the network, we then calculate overall coverage κ as: $\kappa = \frac{\sum_{u \in \mathcal{U}} \kappa_u}{|\mathcal{U}|}$. Because of our population density dataset, we can weight the coverage metric based on population density, giving us a better estimate of the coverage experienced by the population as a whole. Hence, we randomly sample locations throughout the Netherlands, calculating the SNR between each location and the BS serving that location. Each sample is then weighted based on the population density at that location.

Redundancy: To represent the resilience of a network, we also define *redundancy* based on the number of antennas that are able to deliver an SNR higher than SNR_{min} to each user. Redundancy provides an indication of the network's resilience to failures or performance degradation, as users with higher redundancy levels are within the reach of multiple antennas that can serve them adequately. For example, if one antenna fails or experiences poor channel quality, users with higher redundancy levels can still be served by other antennas creating a more resilient network. However, there is a trade-off between redundancy and power consumption, as increasing redundancy typically requires deploying more antennas and BSs, which in turn increases the overall power consumption of the network. For each user $u \in \mathcal{U}$, we calculate the redundancy level R_u as the number of BSs $b \in \mathcal{B}$ such that there exists an antenna a

[4]We also had to filter out the antennas used only for maritime communications by TampNet and fix the non-consistent use of comma separator for both 1000 separator and decimal separator.

belonging to BS b that provides sufficient SNR to user u. Thus, we define the redundancy level R_u for user u as follows:

$$R_u = |\{b \in \mathcal{B} \mid \exists a \in \mathcal{A}_b : SNR_{a,u} > \text{SNR}_{\text{min}}\}|. \quad (5)$$

Consequently, the overall population-weighted redundancy R_{pop} of the setting is calculated as a weighted average of sampled location redundancies across the country considering the population density. More formally, for all sampled locations denoted by $\mathcal{S}$, with weights w_s and redundancies R_s, we calculate R_{pop} as follows:

$$R_{pop} = \frac{\sum_{s \in S} w_s \times R_s}{\sum_{s \in S} w_s}. \quad (6)$$

Evaluating the redundancy can be computationally expensive as it requires calculating the SNR between each sampled location and all BSs in the network. Because in the SNR calculation the distance between the location and the BS is a major factor affecting the SNR, we optimize the redundancy evaluation by only considering BSs within a certain radius from each sampled location. This radius is determined based on the maximum distance at which a BS can provide sufficient SNR under ideal conditions (i.e., only free space path loss) with a safety margin of 10% of this distance added.

Power consumption: As the RAN components are responsible for a majority of the energy consumption in mobile networks [18], we consider the energy consumption of the RAN only. Also, the core networks of the MNOs will remain intact in both scenarios studied, hence we leave the core network out in our study. In line with the changes in RAN toward disaggregated architectures, we assume that a BS consists of a BBU and multiple RRHs connected via fronthaul links. We use power models derived from [18] and [4] resulting in the following equation representing the total power consumption at a BS with N_{TRX} transceivers:

$$P_{BS} = N_{TRX} \times \frac{P_{PA} + P_{RF} + P_{BB}}{(1 - \sigma_{DC}) \times (1 - \sigma_{MS})} \quad (7)$$

where P_{PA} is the power consumption of the power amplifier, P_{RF} is the power consumption of the radio frequency components, and P_{BB} is the power consumption of the baseband unit. Losses incurred by the DC-DC conversion and main supply are accounted for using the σ_{DC} and σ_{MS} parameters respectively.

The power consumed by the power amplifier P_{PA} is a function of the output power P_{out}, the efficiency of the power amplifier η_{PA}, and the feeder loss σ_{feed} and is calculated as:

$$P_{PA} = \frac{P_{out}}{\eta_{PA} \times (1 - \sigma_{feed})}. \quad (8)$$

In (8), P_{out} depends on the maximum output power P_{max} and the load factor ρ which is defined as the ratio of the traffic demand D served by the BS divided by the capacity C of that BS. More formally, we calculate P_{out} as follows:

$$P_{out} = P_{max} \times \rho \text{ where } \rho = \frac{D}{C}. \quad (9)$$

We define the capacity C of a BS to represent the maximum throughput it can offer based on the number of antennas it has operating on each frequency band. For a given $b \in \mathcal{B}$ with set of antennas $\mathcal{A}_b$ operating on frequency bands F, we define the set of antennas operating on frequency band f as $\mathcal{A}_{b,f} = \{a \in \mathcal{A}_b | f_a = f\}$. Then the traffic capacity C (in bit/s) is calculated using Shannon's capacity formula as:

$$\forall b \in \mathcal{B} : C_b = \sum_{f \in F} |\mathcal{A}_{b,f}| \times W_f \times \log_2(1 + SNR_{f,b}), \quad (10)$$

where W_f is the bandwidth of frequency band f and $SNR_{f,b}$ is the signal-to-noise ratio experienced by users served on frequency band f at BS b.

We define the current traffic demand D of a BS based on the population served by that BS (pop_b) and assume a per-user traffic demand of d_{user} with an activity factor α_{user} representing the fraction of users that are active at any given time. Then the traffic demand in bits per second D is calculated as:

$$\forall b \in \mathcal{B} : D_b = pop_b \times d_{user} \times \alpha_{\text{user}}. \quad (11)$$

Carbon emissions: We estimate the carbon emissions of the network in two parts: operational and embodied carbon emissions. The operational carbon emissions are calculated based on the energy consumption of the network during its operation and the carbon intensity of the electricity grid. The embodied carbon emissions are associated with the production, transportation, installation, maintenance, and end-of-life disposal of the network equipment. In this paper, we focus on the production and end-of-life disposal phases as these two factors account for the majority (e.g., according to [26], 3586 kg CO_2 for BS production vs. 59.29 CO_2 for transport) of the embodied emission and due to the availability of data only for these phases.

For operational carbon emissions, we calculate the total energy consumption E^{total} of the network for a time period T using power consumption model for each BS in (7). We then use the average carbon intensity (CI) of the Dutch electricity grid to estimate the operational carbon emissions as follows:

$$\text{CO}_2^{\text{operational}} = E^{\text{total}} \times \text{CI}. \quad (12)$$

For embodied emissions, we focus on the following components of a 4G BS: BBU, BBU cabinet, power supply unit (PSU), battery cabinet, batteries, RRU, and antennas. We omit other parts such as backhaul equipment, core network equipment, or site infrastructure such as towers. Each BS has one battery cabinet containing batteries, one BBU cabinet containing the BBU and three PSUs, and one RRU for each antenna. For each component, we collected data on its mass, service life, and emission factors for production and end-of-life disposal from vendor data sheets and literature. Using this data, we estimate the annual embodied carbon emissions of a BS as follows:

$$\text{CO}_2^{\text{embodied}} = \sum_{c \in \mathcal{E}} \frac{m_c \times (f_c^{\text{prod}} + f_c^{\text{eol}})}{L_c}, \quad (13)$$

where $\mathcal{E}$ is the set of components considered, m_c is the mass of component c, f_c^{prod} is the emission factor for the production of component c in kg CO_2 per kg, f_c^{eol} is the emission factor

TABLE II: Emission factors, service life, and mass of network components.

Equipment type	Emission Factor	Mass (kg)	Service life (years)	Source
Base Band Unit (BBU3900)	34.45 kg CO_2/kg	7 [20]	10	Ecoinvent 3.7. Router, internet
BBU Cabinet (APM30H)	4.04 kg CO_2/kg	72 [21]	10	Ecoinvent 3.7. Chassis, internet access equipment
PSU (3x R4850G2)	33.3 kg CO_2/unit	2 [22]	10	Ecoinvent 3.7. Power supply unit, for deskop computer
Battery cabinet	4.04 kg CO_2/kg	70 [23]	10	Ecoinvent 3.7. Chassis, internet access equipment
Batteries	89.98 kg CO_2/kg	10 [23]	10	Ecoinvent 3.7. Router, internet
Remote Radio Unit (RRU3908)	34.45 kg CO_2/kg	15 [24]	10	Ecoinvent 3.7. Router, internet
Antenna (AAU3911)	34.45 kg CO_2/kg	49 [25]	10	Ecoinvent 3.7. Router, internet

for the end-of-life disposal of component c in kg CO_2 per kg, and L_c is the service life of component c in years.

Finally, we calculate the total annual carbon emissions as the sum of the operational and embodied carbon emissions considering all BSs in the infrastructure as follows: $CO_2^{\text{total}} = CO_2^{\text{operational}} + CO_2^{\text{embodied}}$.

We use emission factors per kg of equipment to estimate the embodied carbon emissions, these emission factors differ between equipment types and are based on life cycle assessments. We have selected a set of components per BS to include in our analysis: Base Band Unit (BBU3900), BBU Cabinet (APM30H), Power Supply Unit (3x R4850G2), Battery cabinet, Batteries, Remote Radio Unit (RRU3908), Antenna (AAU3911). We assume that one RRU is required per antenna. While calculating the embodied carbon emissions per BS, we use the number of antennas in our dataset to scale the emissions accordingly.

Table II shows the production emission factors for each type of equipment as well as their lifetime and mass. In addition to these values, we use also the following components for the last step of the lifecycle [23]: (i) dismantling and EoL of ICT equipment with 1.413 kg CO_2/kg, (ii) dismantling and EoL of electronic component with 0.310 kg CO_2/kg, and battery EoL with 1.65 kg CO_2/kg. In our analysis, we consider the PSUs as electronic component, while all other radio components are considered ICT equipment.

V. Neutral Host Network (NHN) Construction

In this section, we introduce our approach to construct a hypothetical NHN. As current MNOs have already optimized the locations of their BSs with careful considerations of the landscape and urban environment, we construct the NHN based on the existing BS locations and selecting a subset of the BSs in the current MNOs. While this approach ensures that the location of the merged BS is realistic and has already been deemed suitable for mobile network coverage, it does not provide the optimal NHN deployment which is beyond the scope of our paper.

Given a set of MNOs $\mathcal{M} = \{M_1, M_2, \ldots, M_N\}$, each MNO M_i operates its own set of BSs $\mathcal{B}^{M_i}$ and antennas $\mathcal{A}^{M_i}$. We denote the set $\mathcal{B} = \bigcup_{i=1}^{N} \mathcal{B}^{M_i}$ as the combined set of all existing BSs from all MNOs. To construct the NHN, we select a subset of BSs $\mathcal{B}^{NH} \subseteq \mathcal{B}$ to be included in the NHN adopting a two-step process: (i) *clustering*: first we cluster the BSs based on their geographic proximity and demand served, then (ii) *merging*: we merge the BSs in each cluster into a single NHN BS while ensuring that the selected BSs can meet the traffic demand. Next, we introduce each step.

A. Cluster-based NHN construction

To identify the regions with high BS density which will act as potential locations to decrease the network redundancy, we first cluster BSs for all MNOs based on geographic proximity limited by a distance threshold d_{thresh}. We choose one BS as the seed of a new cluster, then all BSs within distance d_{thresh} of that BS are added to the cluster, as long as the combined traffic demand of the BSs in the cluster does not exceed a predefined load threshold $\rho_{\max}$ when merged. This process is repeated until all BSs have been assigned to a cluster.

As Alg.1 (Line 2) shows, we select as the seed of a new cluster (b_{seed}) the BS with the highest population served among the unassigned BSs. We then go through all neighbours of the seed BS that are within the distance threshold d_{thresh} (Line 3), starting from the closest one (Line 4) to evaluate whether to add each neighbour in $\mathcal{N}$ to the cluster (Line 6).

When considering whether to cluster two BSs together or to add a BS to an existing cluster, we evaluate the combined demand of the BSs in the cluster. For an existing cluster γ_k and a candidate BS b_{new}, we calculate the total demand D_{γ_k} of the cluster including the new BS as the sum of traffic demand of the cluster and the new BS (Line 7) as $D_{\gamma_k} = D_{b_{new}} + \sum_{b \in \gamma_k} D_b$.

To ensure that the NHN can satisfactorily serve the traffic demand of the users, we need to consider the total capacity of the NHN BS that would result from merging the BSs in the cluster (Line 8). For merging the BSs, we develop also a heuristic listed in `BuildMergedBS` (Alg. 2) which constructs a merged NHN BS from a cluster of existing BSs. `MergedCapacity` (Alg. 3) computes the capacity of a merged NHN BS. If the load factor $\rho_{\gamma_k} = \frac{D_{\gamma_k}}{C_{\gamma_k}}$ of the merged BS would exceed ρ_{max}, we do not add the new BS to the cluster (Line 9). Here, C_{γ_k} is the total capacity of the merged BS given by (10). This capacity depends on the spectral efficiency experienced by the users served by the antennas of the merged BS. Before we start our clustering process we precompute the spectral effiency for all antennas in the dataset using the SNR model in Sec. III-B. We then use the mean of the spectral efficiencies of all antennas in the cluster to estimate the capacity of the merged BS. If adding b to the cluster keeps the load factor $\rho' = \frac{D'}{C_{\text{cap}}}$ within the limit, we add b to the cluster and update the total demand D' of the cluster (Line 10). This process is continued until the neighbouring BSs have all been evaluated and either added to the cluster or skipped. This clustering process is repeated until

Algorithm 1 ClusterBSs

Require: Set of BSs $\mathcal{B}$ with positions $\text{pos}(b)$ and demand D_b, distance threshold d_{thresh}, load limit $\rho_{\max}$
Ensure: Set of clusters $\Gamma = \{\gamma_1, \ldots, \gamma_K\}$ where $\forall \gamma \in \Gamma : \gamma \subseteq \mathcal{B}$, $\mathcal{B}_0 \leftarrow \mathcal{B}$, $\Gamma \leftarrow \emptyset$

while $\mathcal{B}_0 \neq \emptyset$ **do**
  $b_{\text{seed}} \leftarrow \arg\max_{b \in \mathcal{B}_0} D_b$
  $\mathcal{N} \leftarrow \{b \in \mathcal{B}_0 \mid \|\text{pos}(b) - \text{pos}(b_{\text{seed}})\| < d_{\text{thresh}}\}$
  Sort $\mathcal{N}$ in ascending order of $\|\text{pos}(b) - \text{pos}(b_{\text{seed}})\|$
  $\gamma \leftarrow \{b_{\text{seed}}\}$ and $D_\gamma \leftarrow D_{b_{\text{seed}}}$
  for $b \in \mathcal{N} \wedge b \neq b_{\text{seed}}$ **do**
    $\gamma' \leftarrow \gamma \cup \{b\}$ and $D'_\gamma \leftarrow D_\gamma + D_b$
    $C'_\gamma \leftarrow \text{MergedCapacity}(\gamma')$ and $\rho'_\gamma \leftarrow \dfrac{D'_\gamma}{C'_\gamma}$
    if $\rho'_\gamma \leq \rho_{\max}$ **then**
      $\gamma \leftarrow \gamma'$ and $D_\gamma \leftarrow D'_\gamma$
  $\mathcal{B}_0 \leftarrow \mathcal{B}_0 \setminus \gamma$ and $\Gamma \leftarrow \Gamma \cup \{\gamma\}$
return Γ

all BSs have been assigned to a cluster, resulting in the final set of clusters $\Gamma = \{\gamma_1, \gamma_2, \ldots, \gamma_K\}$ of K clusters.

B. Merged BS and capacity calculation

In Alg. 2, we construct a merged NH BS from a cluster of existing BSs. In this process, there are two key steps: (i) selecting the location of the merged BS and (ii) selecting the antennas to be included in the merged BS. The location of the final neutral host BS is chosen as the location of the BS in the cluster with the maximum number of antennas: $b_{\text{rep}} = \arg\max_{b \in \gamma} |\mathcal{A}_b|$. We chose this heuristic as BSs with more antennas likely have the available space and structural support to host a larger number of antennas that is required for the merged BS. Additionally, a BS with more antennas is deemed a suitable location by the original operator, indicating that it is likely a good location for coverage and capacity.

When selecting the antennas to be included in the merged BS, we first combine all antennas from all BSs in the cluster. Because typically multiple BSs in a cluster operate on the same frequency band. Hence, this approach leads to an excessive number of antennas operating on the same frequency band. As having too many antennas operating on the same frequency band in close proximity can lead to interference issues, we limit the number of antennas per frequency band to a maximum of three, as is common practice in sectorized BSs. If more than three antennas in the cluster operate on the same frequency band, we select the three antennas with the highest transmit power to be included in the merged BS. If there is a tie in transmit power, we select the antennas of the BS with the larger number of total antennas.[5]

Alg. 3 computes the capacity of a merged BS which is calculated as in (10), where we sum the capacities contributed

[5]To speed up the processing time of this algorithm, we use a KD-tree data structure to efficiently query neighbouring BSs within d_{thresh}. This allows us to avoid evaluating all BSs when searching for neighbours, significantly reducing the computational complexity of the clustering process.

Algorithm 2 BuildMergedBS

Require: Cluster γ; each $b \in \gamma$ has antenna set $\mathcal{A}_b$
Ensure: Merged NH BS NH_b with antenna set $\mathcal{A}_{NH}$

$b_{\text{rep}} \leftarrow \arg\max_{b \in \gamma} |\mathcal{A}_b|$
$\mathcal{A}_{\text{cluster}} \leftarrow \bigcup_{b \in \gamma} \mathcal{A}_b$
$\mathcal{F} \leftarrow \{f(a) \mid a \in \mathcal{A}_{\text{cluster}}\}$
$\mathcal{A}_{NH} \leftarrow \emptyset$
for $f \in \mathcal{F}$ **do**
  $\mathcal{A}_f \leftarrow \{a \in \mathcal{A}_{\text{cluster}} \mid f(a) = f\}$
  if $|\mathcal{A}_f| \leq 3$ **then**
    $\mathcal{A}_{NH} \leftarrow \mathcal{A}_{NH} \cup \mathcal{A}_f$
  else
    Sort $\mathcal{A}_f$ by descending: (i) $P_{\text{tx}}(a)$ and (ii) $|\mathcal{A}_{\text{bs}(a)}|$
    $\mathcal{A}_{NH} \leftarrow \mathcal{A}_{NH} \cup \{\mathcal{A}_{f,1}, \mathcal{A}_{f,2}, \mathcal{A}_{f,3}\}$
Create NH_b with:
  $\text{pos}(NH_b) \leftarrow \text{pos}(b_{\text{rep}})$ and $\mathcal{A}_{NH}(NH_b) \leftarrow \mathcal{A}_{NH}$
return NH_b

Algorithm 3 MergedCapacity

Require: Merged NH BS NH_b with antenna set $\mathcal{A}_{NH}$
Ensure: Total capacity C_{cluster}

$C_{\text{cluster}} \leftarrow 0$ and $\mathcal{F} \leftarrow \{f(a) \mid a \in \mathcal{A}_{NH}\}$
for each frequency band $f \in \mathcal{F}$ **do**
  $\mathcal{A}_{NH,f} \leftarrow \{a \in \mathcal{A}_{NH} \mid f(a) = f\}$
  $N_{TRX,f} \leftarrow |\mathcal{A}_{NH,f}|$ and $B \leftarrow 20$ MHz
  $SE_f \leftarrow \dfrac{\sum_{a \in \mathcal{A}_{NH,f}} SE_a}{|\mathcal{A}_{NH,f}|}$
  $C_{\text{cluster}} \leftarrow C_{\text{cluster}} + N_{TRX,f} \cdot B \cdot SE_f$
return C_{cluster}

by each frequency band f covered by the merged BS. The bandwidth B is assumed to be 20 MHz for all frequency bands, and the spectral efficiency SE_f is calculated as the mean of the spectral efficiencies of all antennas operating on frequency band f. Note that this spectral efficiency is precomputed for all antennas in the dataset before starting the clustering process, using the SNR model outlined in Section III-B, thus the final spectral efficiency will likely be lower than the mean due to increased distance between the merged BS and the users it serves. Our algorithm runs in polynomial time as Alg.1 has worst-case complexity of $O(|\mathcal{B}|^2 \times |\mathcal{F}|)$.

VI. Performance Evaluation

Now, we evaluate the performance of the NHN using our in-house Python simulator and compare NHN against current mobile networks deployed separately by individual MNOs. Moreover, we adopt three NHN scenarios that have different d_{thresh} and $\rho_{\max}$ values. We refer to them as optimistic, moderate, and conservative to reflect their NHN construction approaches and we set the parameters as follows:

- **Optimistic** with $d_{thresh} = 1000$m and $\rho_{max} = 0.9$,
- **Moderate** with $d_{thresh} = 500$m and $\rho_{max} = 0.7$,
- **Conservative** with $d_{thresh} = 200$m and $\rho_{max} = 0.5$.

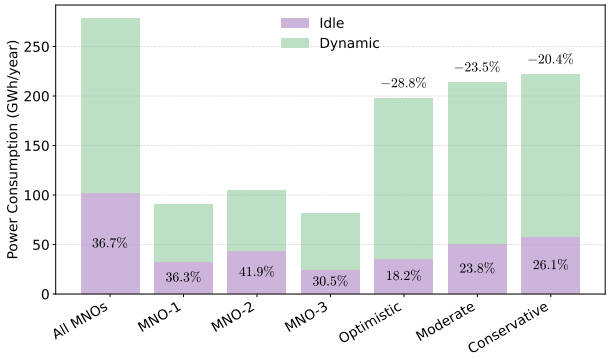

(a) Power consumption (idle and load-dependent dynamic power).

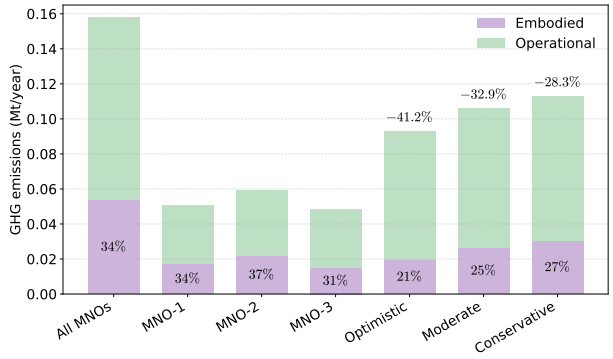

(b) Carbon emissions (embedded and operational).

Fig. 3: Power consumption and carbon emissions for individual MNOs, all MNOs jointly, and various NHN scenarios.

TABLE III: SNR and power model parameters

SNR model parameters		**Power model parameters**	
Parameter	Value	Parameter	Value
P_{TX}	38 dBm [27]	σ_{feed}	0.2
G_{TX}, G_{RX}	18 dB, 0 dB [28]	σ_{cool}	0
Bandwith B	20 MHz [27], [28]	σ_{DC}	0.075
NF	5 dB [28]	σ_{MS}	0.09
h_{UT}	1.5 m [27]	P_{RF}	12.9 W
h (UMa)	25 m [27]	P_{BB}	29.6 W
h (RMa)	5 m [27]	η_{PA}	0.311
Street width	10 m [29]	P_{max}	4 W per DL MHz
f_c, h_{BS}	from antenna data	d_{user}	1 Mbps
α_{active}	0.05	CI	0.388 kg CO_2/kWh

These d_{thresh} values are chosen after analyzing the current MNOs' inter-site distances.[6] Table III lists the default values of the key parameters that are kept the same across our evaluations unless otherwise stated.

A. Power consumption and carbon emissions

Fig. 3a presents the resulting total power consumption for each MNO, the national cellular infrastructure's consumption (marked as All MNO in the figures), and three NHN scenarios. The figure shows also the break down of the power consumption into idle power consumption (the static power to keep the BS site on) and load-dependent dynamic power. The percentage in each idle power bar indicates the percentage of the total power consumption of that MNO/scenario due to idle power consumption. On top of each bar for the NHN scenarios, we also indicate the percentage reduction in power consumption compared to all MNOs. From the figure, we can observe that the NHN scenarios have significantly lower power consumption compared to the combined individual MNOs, ranging from approximately 20% to 28% reduction depending on the scenario. As expected, the optimistic scenario has the lowest power consumption, followed by the moderate and conservative scenarios. The improvement in power consumption is due to the decreased number of BSs (shown in Fig.4a) and hence saving from the idle power. Our analysis shows that NHN deployments can decrease the number of BSs significantly (e.g., 67% for optimistic scenario). Zooming in the NHN scenarios, we also observe that the power consumption of the NHN scenarios is divided differently into idle and dynamic power consumption than that of individual MNOs (e.g., 26.1% for Conservative NHN scenario whereas it is 36.7% for All MNOs). This is expected as the resulting infrastructure has fewer BSs in NHNs (Fig.4a), but serves a higher load on each BS (Fig. 4c).

In addition to this lower operational power consumption, NHNs also provide benefits in embodied carbon emissions due to fewer BSs in the infrastructure. As Fig.3b depicts, NHN scenarios lead to a significant reduction in annual carbon emissions compared to the individual MNOs; the reduction ranges from 28.3% to 41.2% depending on the scenario. Another observation is that the embodied annual emissions account for a larger portion for the individual MNOs compared to the NHN scenarios. This is expected as the NHN has fewer BSs, leading to a lower share of embodied emissions compared to operational emissions due to running the BSs at a higher load as discussed next.

Fig.4 shows the number of BSs, antennas, and the load distribution across the existing BSs. We can see as expected that the optimistic scenario achieves the highest reduction, with a 67% fewer BSs and over 64% fewer antennas. As we move to the moderate and conservative scenarios, the relative decrease is smaller with the conservative scenario achieving the lowest reduction of 44% fewer BSs and around 43% fewer antennas. Notice that the reduction in number of antennas is higher than the reduction in the number of BSs due to our approach to keep maximum three antennas per frequency band while merging BSs. If any of the BSs in the cluster had more than 3 antennas for a given band, this leads to a larger reduction in the total number of antennas compared to the number of BSs. Finally, Fig.4c depicts the load distribution across BSs which corroborates our argument on increased dynamic power consumption due to higher average load. Despite this increase in load, we can observe that MNOs still have ample capacity as load is typically low due to highly overprovisioned resources.

[6]We also evaluated the impact of these two parameters which are omitted in this paper for the sake of space. However, they can be accessed from [1].

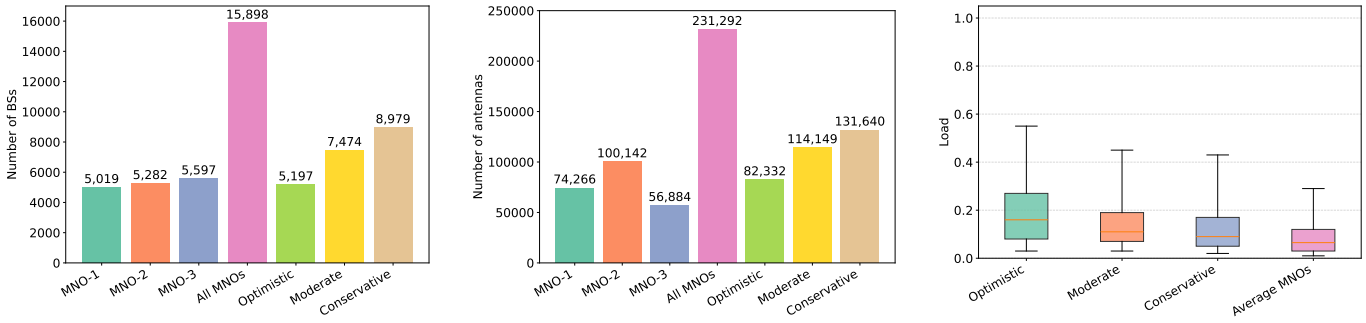

(a) Number of BSs in the infrastructure.

(b) Number of antennas in the infrastructure.

(c) BS load.

Fig. 4: Total number of (a) BSs and (b) antennas, and (c) BS load in each scenario.

Key insight: NHN deployments can decrease operational power consumption by decreasing the idle power consumption in the network due to the reduced number of BSs. Moreover, lower number of BSs leads to reduction in the embodied carbon emissions. Consequently, depending on the NHN scenario, total carbon emission reduction can be up to 41.2% while observed power consumption decrease can be up to 28.8%.

B. Coverage and signal quality analysis

While NHN scenarios are shown to facilitate significant sustainability improvements, they might affect coverage, signal quality, and redundancy as a result of sparser BS deployment. While Alg.2 ensures that the traffic demand from the users can still be satisfied by the NHN, the observed signal quality might deteriorate resulting in potential performance issues. Hence, let us analyze the impact of reduced number of BSs on the signal quality and consequently coverage.

Fig. 5 shows the SNR distribution for each MNO as well as the three NHN scenarios. We also record the percentage of users experiencing an SNR below 7 dB to reflect coverage gaps. These values are: [0.12%, 0.01%, 0.13%, 0.74%, 0.17%, 0.18%, 0.20%] in the order of the scenarios presented in Fig.5. The SNR values are weighted based on the population density in each grid cell to reflect the user experience. Fig.5 shows that NHN scenarios have a lower median SNR compared to the individual MNOs, as well as a more spread out distribution. This indicates that while the average user experience in terms of SNR is lower across all scenarios, there are more users experiencing both very high and very low SNR values in the NHN scenarios.

From conservative to the optimistic scenario, the median SNR decreases further, and the spread of the distribution decreases. As we move to more aggressive clustering, the distance between BSs increases leading to larger areas with lower signal strength highlighting the importance of the trade-off between network simplification (consequently environmental footprint) and coverage and signal quality. Please note that while NHNs typically lead to lower SNR values, it is only a small fraction of users that do not maintain a signal quality of 7 dB, e..g, less than 0.2% for Optimistic which is still higher than MNO-3. Hence, our observation is that network coverage is only marginally degraded with the majority of users experiencing acceptable signal quality.

To investigate potential causes of low SNR values, we analyze the SNR statistics per EARTH E3F density class. Fig. 6 presents the difference in mean SNR per density class for NHN scenarios compared to the conventional isolated MNOs. The difference in mean SNR for scenario X for each density class is calculated as follows: $\Delta\text{SNR}_X = \text{SNR}_X - \frac{1}{3}\sum_{i=1}^{3}\text{SNR}_{MNO_i}$ where SNR_{MNO_i} is the SNR for MNO i for that density class. This allows us to compare the SNR of NHN scenarios and the MNOs on a per-density class basis. From Fig.6, we can observe that the mean SNR for the optimistic scenario is lower than the average of the MNOs across all density classes, with the largest decrease in `Super dense urban areas`. This could be caused by the fact that there are very few super dense urban areas in the Netherlands, the average number of BSs serving a super dense urban area is only 19 for the individual MNOs. When we merge BSs, any BS located in one of these areas are likely to be merged with BSs located in lower-density areas nearby, leading to a decrease in signal quality for users in the super dense urban areas. As we move to the moderate and conservative scenarios, the mean SNR improves but is still lower than the MNO average, except for `Dense Urban` and `Super Dense Urban` classes. For urban areas, the mean SNR is 1.8 dB to 1.3 dB lower than the MNO average for the moderate and conservative scenarios, respectively. We infer from these results that different areas might be affected differently depending on their density class and hence an NHN deployment approach should consider the density class of each region while determining its BS deployment. For example, rather than applying a fixed d_{thresh}, our algorithm could consider a dynamic threshold value that varies based on the density class of the BSs being considered for merging and more aggressive merging could be applied in higher-density areas while being more conservative in lower-density areas to maintain coverage. Moreover, for attaining a balance between coverage and environment footprint, a setting similar to the conservative scenario should be preferred rather than the optimal scenario.

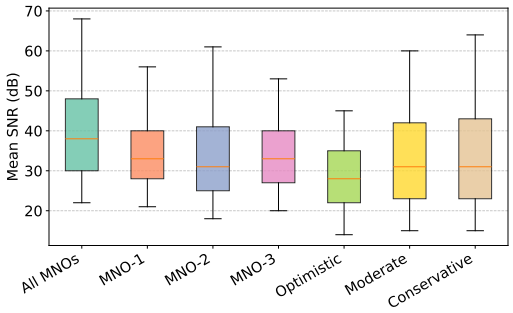

Fig. 5: SNR distribution for the studied scenarios.

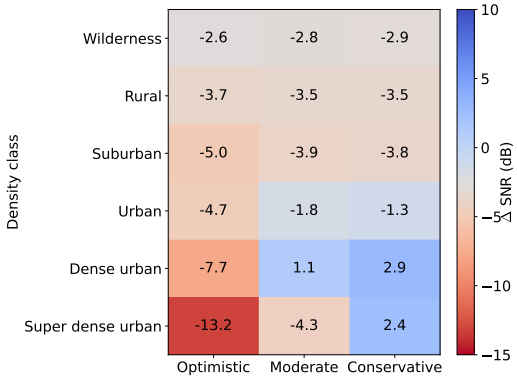

Fig. 6: SNR difference for each density class.

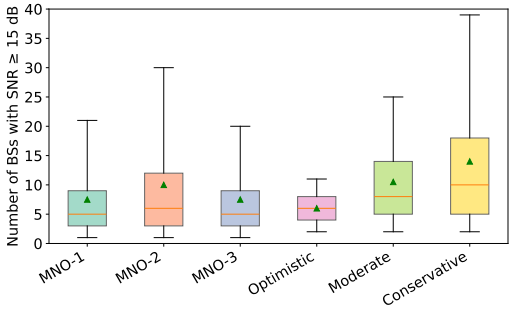

Fig. 7: # of BSs covering each user with a 15 dB SNR threshold.

Key insight: Due to the decreased number of BSs, the signal quality decreases slightly under NHNs. However, this decrease does not lead to coverage loss as the maintained SNR is still above an acceptable minimum quality. Moreover, merging approach should be more dynamic and take into the density class of each region.

C. Resilience analysis

As presented in Sec.III, we introduced redundancy, defined as the number of BSs that provide coverage to each user above a certain SNR threshold, as a proxy of resilience of the cellular infrastructure. Fig. 7 presents the distribution of the number of BSs covering each user for $\text{SNR}_{\text{min}} = 15\,\text{dB}$. We can observe that the optimistic scenario provides similar redundancy compared to the individual MNOs, while the moderate and conservative scenarios provide higher redundancy. This is a consequence of the denser deployment of BSs in these scenarios, as more BSs are retained due to the more conservative clustering parameters. We can also see that for both SNR thresholds the NHN has a higher fifth percentile compared to the individual MNOs, indicating that even though more users experience lower SNR values in NHN scenarios, they still benefit from having multiple BSs providing coverage. In case of disruption of the serving BS (e.g., hardware or software-related failures or planned maintenance), there are many BSs in proximity that can provide high signal quality.

VII. Limitations and Future Work

The key limitations of our work can be listed as follows: (i) interference not considered, (ii) load and capacity models not reflecting the spatio-temporal dynamics of mobile traffic, (iii) neutral host deployment approach, and (iv) future scenarios. To keep our analysis tractable and for a nation-wide analysis, we considered only SNR ignoring the impact of interference from the neighboring co-channel BSs. While we expect this simplification lead to optimistic values of SNR, current MNOs apply many approaches for interference mitigation, e.g., coordinated multi-point access. That being said, we foresee that interference could be incorporated into our modeling with simplifying assumptions, e.g., only nearest BSs resulting in interference. Second, our analysis does not have temporal dimension; e.g., constant load based on the population of an area. However, unsurprisingly, traffic load follows human activity patterns, e.g., mobility, work hours, which changes over time and space. Hence, expanding our models and analysis with temporal dynamics is another future direction. To represent an NHN, we developed a heuristic assuming that the NHN will be constructed based on the current infrastructure. While this is a realistic assumption, we expect that future NHNs can be optimized in many ways, including the location of the BSs, their antenna orientations, frequencies, to name a few. With such optimizations, the benefits of NHN deployments would likely be higher. Finally, as 5G networks are soon ubiquitously deployed, our analysis should be adapted to 5G network with appropriate models for operational and embodied emissions. Moreover, future scenarios, e.g., grid decarbonization affecting carbon intensity or traffic increase in mobile networks, need to be considered in carbon emission calculations.

VIII. Conclusions

This work investigated the potential of neutral host deployments in decreasing the carbon emissions of a nation-wide cellular infrastructure by decreasing the number of BSs and allowing multiple mobile network providers to utilize the neutral host resources with higher utilization. Our data-driven analysis for the Netherlands has shown significant benefits in decreasing carbon emissions, e.g., up to ∼41%, without a significant loss in coverage, signal-quality, and resilience.

Acknowledgment

This work is supported by the National Growth Fund through the Dutch 6G Flagship Project "Future Network Services".

References

[1] B. Gerretzen, "Optimizing mobile networks for sustainability: A study on neutral host architectures," Master's thesis, University of Twente, Enschede, Netherlands, 2026. [Online]. Available: https://purl.utwente.nl/essays/109367

[2] L. Golard, J. Louveaux, and D. Bol, "Evaluation and projection of 4g and 5g RAN energy footprints: the case of belgium for 2020–2025," vol. 78, no. 5, pp. 313–327. [Online]. Available: https://doi.org/10.1007/s12243-022-00932-9

[3] Next G Alliance, "Green G: The Path Towards Sustainable 6G ," 2022, https://nextgalliance.org/white_papers/green-g-the-path-towards-sustainable-6g/?dl=19802008.

[4] A. Ahmed and M. Coupechoux, "The long road to sobriety: Estimating the operational power consumption of cellular base stations in france," in *2023 International Conference on ICT for Sustainability (ICT4S)*. IEEE, pp. 188–196. [Online]. Available: https://ieeexplore.ieee.org/document/10292167/

[5] L. Mata, M. Sousa, P. Vieira, M. P. Queluz, and A. Rodrigues, "Optimizing energy and spectral efficiency in mobile networks: A comprehensive energy sustainability framework for network operators," *IEEE Access*, vol. 13, pp. 22 342–22 364, 2025.

[6] E. J. Oughton, J. Oh, S. Ballan, and J. Kusuma, "Sustainability assessment of 4G and 5G universal mobile broadband strategies," 2023. [Online]. Available: https://arxiv.org/abs/2311.05480

[7] N. L. Omnes, C. Adam, A. Braud, F. Latron, L. le Beller, and B. Radier, "How to favour more cooperative deployments for network infrastructures," in *10th International Conference on ICT for Sustainability (ICT4S)*, 2024, pp. 162–171.

[8] L. Finarelli, M. Ni, M. Meo, F. Dressler, and G. Rizzo, "Sharing is caring: Analysis of hybrid network sharing strategies for energy efficient multi-operator cellular systems," in *IEEE International Conference on Modeling, Analysis and Simulation of Wireless and Mobile Systems (MSWiM)*, 2025, pp. 128–133.

[9] R. Bajracharya, R. Shrestha, H. Jung, and H. Shin, "Neutral host technology: The future of mobile network operators," *IEEE Access*, vol. 10, pp. 99 221–99 234, 2022.

[10] A. Antonopoulos, E. Kartsakli, A. Bousia, L. Alonso, and C. Verikoukis, "Energy-efficient infrastructure sharing in multi-operator mobile networks," *IEEE Communications Magazine*, vol. 53, no. 5, pp. 242–249, 2015.

[11] L. Bonati, M. Polese, S. D'Oro, S. Basagni, and T. Melodia, "NeutRAN: An open RAN neutral host architecture for zero-touch RAN and spectrum sharing," vol. 23, no. 5, pp. 5786–5798. [Online]. Available: https://ieeexplore.ieee.org/abstract/document/10238780

[12] D. Renga, M. Meo, and L. Nuaymi, "Network sharing: a pathway to sustainability and carbon footprint mitigation in radio access networks," in *36th International Teletraffic Congress (ITC-36)*. IEEE, 2025.

[13] L. Golard, Y. Agram, F. Rottenberg, F. Quitin, D. I. D. Bol, and J. Louveaux, "A parametric power model of multi-band sub-6 ghz cellular base stations using on-site measurements," *2024 IEEE 35th International Symposium on Personal, Indoor and Mobile Radio Communications (PIMRC)*, pp. 1–7, 2024. [Online]. Available: https://api.semanticscholar.org/CorpusID:275176346

[14] Y. Zhong and X. Ge, "Toward 6G carbon-neutral cellular networks," *IEEE Network*, vol. 38, no. 5, pp. 174–181, 2024.

[15] European Telecommunications Standards Institute, "TR 138 901 - v19.1.0 - 5g; study on channel model for frequencies from 0.5 to 100 GHz (3gpp TR 38.901 version 19.1.0 release 19)."

[16] Frequenties voor mobiele netwerken. [Online]. Available: https://antennekaart.nl/page/frequencies

[17] WorldPop,, Center for International Earth Science Information Network (CIESIN), and Columbia University, "The spatial distribution of population density in 2020, netherlands." [Online]. Available: https://www.worldpop.org/doi/10.5258/SOTON/WP00674

[18] G. Auer, V. Giannini, C. Desset, I. Godor, P. Skillermark, M. Olsson, M. A. Imran, D. Sabella, M. J. Gonzalez, O. Blume, and A. Fehske, "How much energy is needed to run a wireless network?" vol. 18, no. 5, pp. 40–49. [Online]. Available: https://ieeexplore.ieee.org/document/6056691

[19] M. Olsson, S. Tombaz, I. Gódor, and P. Frenger, "Energy performance evaluation revisited: Methodology, models and results," in *2016 IEEE 12th International Conference on Wireless and Mobile Computing, Networking and Communications (WiMob)*, pp. 1–7. [Online]. Available: https://ieeexplore.ieee.org/document/7763182/

[20] Huawei, "BBU3900 description." [Online]. Available: https://actfornet.com/ueditor/php/upload/file/20200526/1590433716257194.pdf

[21] ——. Apm30h tmc11h ibbs installation guide. [Online]. Available: https://www.scribd.com/doc/128584941/apm30h-tmc11h-ibbs-installation-guide-pdf

[22] ——, "R4850g2 rectifier data sheet." [Online]. Available: https://www.cdiweb.com/datasheets/huawei/r4850g2%20rectifier%20data%20sheet%2005-.pdf

[23] D. Ruiz, G. San Miguel, J. Rojo, J. Teriús-Padrón, E. Gaeta, M. Arredondo, J. Hernández, and J. Pérez, "Life cycle inventory and carbon footprint assessment of wireless ICT networks for six demographic areas," vol. 176, p. 105951. [Online]. Available: https://linkinghub.elsevier.com/retrieve/pii/S0921344921005607

[24] Huawei, "RRU3908 description." [Online]. Available: https://cosconor.fr/GSM/Divers/Equipment/Huawei/-%20Huawei%20RRU%20(2019)/RRU%203908/Description.pdf

[25] ——. AAU3911 technical specifications. [Online]. Available: https://www.scribd.com/document/593136729/AAU3911-Technical-Specifications-V100R016C10-02-PDF-EN

[26] Y. Zhong and X. Ge, "Toward 6g carbon-neutral cellular networks," pp. 1–1, conference Name: IEEE Network. [Online]. Available: https://ieeexplore.ieee.org/document/10552231/?arnumber=10552231

[27] 3GPP, "TS 36.104 evolved universal terrestrial radio access (e-UTRA); base station (BS) radio transmission and reception." [Online]. Available: https://portal.3gpp.org/desktopmodules/Specifications/SpecificationDetails.aspx?specificationId=2412

[28] National Telecommunications and Information Administration, "LTE (FDD) transmitter characteristics." [Online]. Available: https://www.ntia.gov/sites/default/files/meetings/lte_technical_characteristics_0.pdf

[29] Rijstrook - wegenwiki. [Online]. Available: https://www.wegenwiki.nl/Rijstrook